Empirical Evaluation of Advanced Ear Biometrics

Ping Yan   Kevin W. Bowyer
Department of Computer Science and Engineering
University of Notre Dame, IN 46556

Abstract

We present results of the largest experimental investigation of ear biometrics to date. Approaches considered include a PCA ("eigen-ear") approach with 2D intensity images, achieving 63.8% rank-one recognition; a PCA approach with range images, achieving 55.3%; Hausdorff matching of edge images from range images, achieving 67.5%; and ICP matching of the 3D data, achieving 98.7%. ICP based matching not only achieves the best performance, but also shows good scalability with size of dataset. The data set used represents over 300 persons, each with images acquired on at least two different dates. In addition, the ICP-based approach is further applied on an expanded data set of 404 subjects, and achieves 97.5% rank one recognition rate. In order to test the robustness and variability of ear biometrics, ear symmetry is also investigated. In our experiments around 90% of people's right ear and left ear are symmetric.

Keyword: biometrics, ear biometrics, 3-D shape, principal component analysis, Iterative closest point, Hausdorff distance, ear symmetry.

1 Introduction

Researchers have suggested that the shape and appearance of the human ear is unique to each individual and relatively unchanging during the lifetime of an adult [11]. Therefore, the ear has been proposed for use in biometrics [4, 11, 5, 10]. In fact, the ear may already be used informally as a biometric. For example, the United States Immigration and Naturalization Service (INS) has a form giving specifications for the photograph that indicates that the right ear should be visible [INS Form M-378 (6-92)].

Moreno et al. [12] experiment with three neural net approaches to recognition from 2D intensity images of the ear. Their testing uses a gallery of 28 persons plus another 20 persons not in the gallery. They find a recognition rate of 93% for the best of the three approaches. They consider three methods of combining results of the different approaches - Borda, Bayesian, and weighted Bayesian combination- but do not find improved performance over the best individual method.

PCA (Principal Component Analysis) on 2D intensity images for ear biometrics has been explored by Victor [18] and Chang [5]. The two studies obtained different results when compared with the performance of facial biometrics. Both ear and face show similar performance in Chang's study, while ear performance is worse than face in Victor's study. Chang explained that the difference might be due to differing ear image quality in the two studies.

Yuizono [22] implemented a recognition system for 2D intensity images of the ear using genetic search. In the experiment they had 660 images from 110 persons, with 6 images per person. They reported that the recognition rate for the registered persons was approximately 100%, and the rejection rate for unknown persons was 100%.

Bhanu and Chen presented a 3D ear recognition method using a local surface shape descriptor [3]. The local surface patches are defined by the feature point and its neighbors, and the patch descriptor consists of its centroid, 2D histogram and surface type. There are four majors steps in the method: feature point extraction, local surface description, off-line model building and recognition. Twenty range images from 10 individuals (2 images each) are used in the experiments and a 100% recognition rate is achieved for their dataset. We implemented their method from the description in [3]. Slight differences were determined experimentally: (1) Due to the noisy nature of range data, the feature points are determined by the shape index type instead of the shape index value. (2) Considering the computation time required, comparison of the two local surfaces was done only when their Euclidean distance was less than 40 pixels. This assumption is valid in our dataset. Using two images each from the first 10 individuals in our dataset, we also found a 100% recognition rate. But when we increased the dataset to 202 individuals, the performance dropped to 33% (68 out of 202). The computation time required for this technique was also larger than that for PCA-based and edge-based techniques that we investigated.

In [7], Chen and Bhanu used two-step ICP on a dataset of 30 subjects with 3D ear images. First, the ear helix is au-

tomatically detected using the 3D depth value. Then initial rigid transformation is computed from a coarse alignment between test ear helix and model ear helix. And finally the root mean square registration error is obtained from the second step by using all the points from the ear. They claimed that the experimental results with 2 incorrect matches out of 30 pairs of ear are reached.

Pun and Moon [15] have surveyed the still-relatively-small literature on ear biometrics. They summarized elements of five approaches for which experimental results have been published [5, 10, 3, 4, 22].

Hurley et al. [10] developed a novel feature extraction technique by using force field transformation. Each image is represented by a compact characteristic vector, which is remarkably invariant to initialization, scale, rotation and noise. The experiment displays the robustness of the technique to extract the 2D ear. No ear recognition experimental results were reported in the paper.

The work presented in this paper is unique in several points with respect to prior work. We report results from the largest experimental dataset to date, in terms of number of persons or number of images or number of algorithms considered. Only one other work has considered 3D ear recognition [3], and we compare three other approaches to 3D ear recognition, and find that all exceed the performance of the previous proposed approach. Ours is the first work to consider PCA-based recognition using 3D ear images. Also because we use a large experimental dataset, we are able to explore how the different algorithms scale with dataset size.

2 Data Acquisition

All the images used in this paper were acquired at the University of Notre Dame between October 7, 2003 and December 10, 2004. In each acquisition session, the subject sat approximately 1.5 meters away from the sensor, with the left side of the face facing the Minolta Vivid 910 range scanner. One 640x480 3D scan and one 640 x 480 color image are obtained nearly simultaneously.

The earliest good image for each of 302 persons was enrolled in the gallery. The gallery is the set of images that a "probe" image is matched against for identification. The latest good image of each person was used as the probe for that person. A subset of 202 persons of data was used to explore algorithm options in some initial experiments, and the larger set of 302 persons is used for final experiments. In addition, the ICP-based approach is further applied on an expanded data set of 404 subjects. Images in the gallery are enrolled into the system for identification. Images in the probe set are applied to be matched against those images in the gallery.

3 Preprocessing and Ear Extraction

Data normalization is applied separately on the 2D and 3D data. And the normalized images are used for the PCA and edge-based approaches. The ICP-based approach does not require such extensive normalization. Details of the steps for normalization can be found in [20].

3.1 Landmark Selection

We have investigated three different landmark selection methods. The first method is the two-point landmark described in [5]. The upper point is called the Triangular Fossa, and the lower point is called the Antitragus [11], see Figure 1(a).
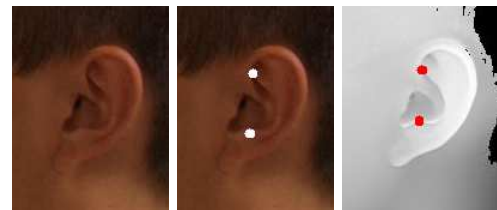
(a) Landmark1: Using Triangular Fossa and Antitragus
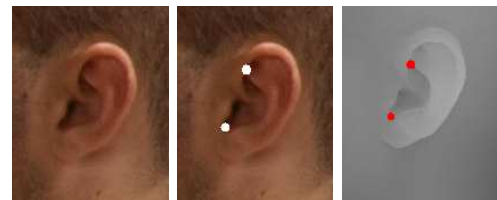
(b) Landmark2: Using Triangular Fossa and Incisure Intertragica
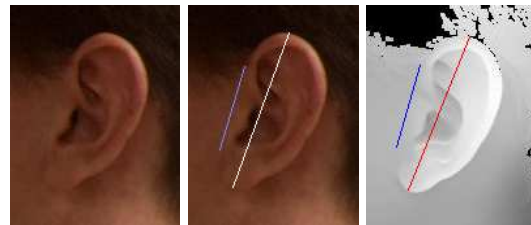
(c) Landmark3: Using Two Lines

Figure 1. Example of Ear Landmarks

The rationale for using landmarks is that the position of the landmark is stable over time for a particular ear. However, these two points are not easily detected in all images. For instance, many ears in our study have a small or subtle Antitragus. The ambiguity in marking this landmark position might affect the ear extraction. Two different points from the Antitragus might be marked on the same ear on two different dates. In order to solve this problem, two other landmark methods were examined. The second one is

similar to the first two-point landmark, but we used the Incisure Intertragica instead of Antitragus as the second point, shown in Figure 1(b). The orientation of the line connecting these two points is used to determine the orientation of the ear, and distance between them is used to measure the size of the ear. But the size of the ear does not have a linear relationship with the distance between these two points. In order to maximize the cropped ear portion, we developed the third method as the two-line landmark, shown in Figure 1(b). One line is along the border between the ear and the face, and the other is from the top of the ear to the bottom. Unlike the two-point landmark, the two-line landmark promises to find most of the ear.

In our experiments, the second method is adopted for further ear extraction in the PCA-based and edge-based algorithms, since it is good at blocking out background and avoiding ambiguity. The two-line landmark is used in the ICP-based algorithm. ICP uses the real 3D range data in the matching procedure and the two matching surfaces should overlap. The two-line landmark gives the opportunity to extract the whole ear for matching, but at the same time, it always includes some background, which increases the background variation, and affects the PCA-based and edge-based performance.

3.2 Ear Extraction

Ear extraction is based on the landmark locations on the original ear images. The original ear images (640 x 480) are cropped to (87x124) for 2D and (68x87) for 3D ears. The 2D ear image has been scaled up for better experimental result, while no scaling is applied on 3D ear range images since the pixel size is constant over different images. The normalized images are masked to "gray out" the background and only the ear is kept.

4 PCA for 2D and 3D Recognition

The PCA (Principal Component Analysis) based approach has been widely used in face recognition [16, 17, 14, 6]. It was also used by Chang [5] in evaluation of 2D ear and face biometrics. In our experiments, a standard PCA implementation [2] is used. Figure 2 shows an example of the images we used for PCA.

For each of the 302 subjects, the earliest good quality 2D and 3D images are used for the 2D and 3D ear space galleries, respectively. The latest good quality images are used as probes. For PCA-based algorithms, eigenvalues and eigenvectors are computed from the images in the training set. In our experiment, the training set is the set of gallery images. The "ear space" is picked out from the eigenvectors corresponding to all the eigenvalues. The best rank-one recognition rate for 2D ear data is 63.6% when dropping
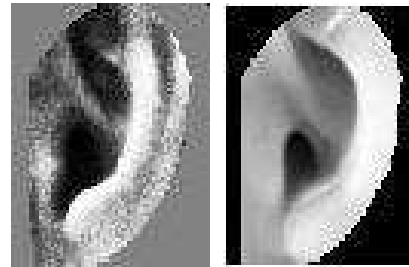
(a) 2D intensity ear   (b) 3D depth value ear

Figure 2. Ear Images As Used For PCA

first 2 and last 23 eigenvectors. The best performance for the 3D ear data is 55.3% when dropping first two eigenvectors. The Yambor Angle [8] distance metric is used. Euclidean distance was tested but gave lower performance.

4.1 2D Ear Data

Two different scalings of the ear sizes are examined on 2D data. One is set as the actual size of the ear, and the other is set at 1.25 times the size of ear. Effectively, this just changes how much of the ear and background appear in the images.

The PCA recognition rate is 66.9% when using 2D regular ear size for 202 subjects. Looking closely at the images created from the eigenvectors associated with 3 largest eigenvalues, it was apparent that each of them had some space behind the contour of ear. Scaling the ear to 1.25 times the original size, the performance increased from 66.9% to 71.4% when using 202 subjects. Using the enlarged ear, the performance is at 63.6% when using 302 subjects, as shown in Figure 5.

Chang obtained 73% rank-one recognition with 88 persons in the gallery and a single time-lapse probe image per person [5]. Our rank one recognition rate for PCA-based ear recognition using 2D intensity images with the first 88 persons is 76.1%, which is similar to the results obtained by Chang, even though we used a different image data set and different landmark points. Thus our 2D ear recognition performance should be representative of the state of the art.
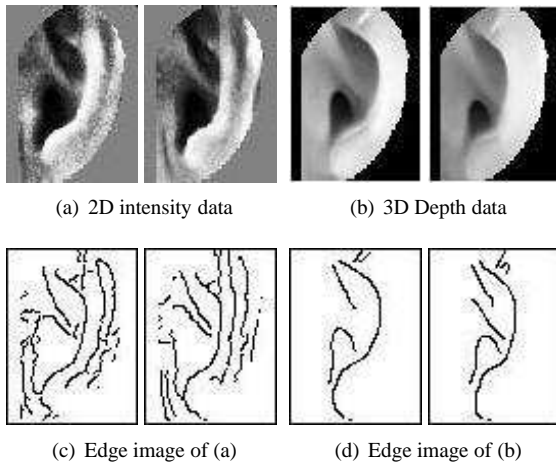
4.2 3D Ear Data

Two different experiments were conducted on the 3D ear data. One is using the original ear range data, the other is applying mean and median filters on the original data to fill the holes of the cropped ear. The performance is improved from 58.4% to 64.8% with hole filling when using 202 subjects. This is still not very good in an absolute sense. One possible reason is that the ear structure is quite complex, and so using mean and median filter alone might not be

good enough to fill holes in the 3D range data. Applying hole filling on the 302 subjects, the performance stays at 55.3% rank one recognition rate, and see Figure 5.

5 Hausdorff Range Edge Matching

Holes in the range data degrade the performance dramatically in the PCA-based approach. Even after we fill holes, the performance is still not as good as we hoped for. After looking carefully at the 2D and 3D data, we noticed that the edge structure in the 3D depth data looks much more stable than in the 2D intensity data.

(a) 2D intensity data   (b) 3D Depth data

(c) Edge image of (a)   (d) Edge image of (b)

Figure 3. Same ear's 2D and 3D Ear Data and Associated Edge Images. Canny Edge Detector Parameters are $sigma = 1.0$, $T_{low} = 0.5$, $T_{high} = 0.5$

Figures 3(a) and 3(b) show the 2D and 3D images taken on two different days of the same person's ear. The Canny edge detector with the same parameters is applied to the 2D and 3D ear data, and the edge images are shown in Figure 3(c) and 3(d). Here, single isolated edge pixels are eliminated from the edge images. It is obvious that edge images of the range image are much cleaner than for the 2D edge images. This is the motivation to develop an edge-based Hausdorff distance method for 3D ear recognition using the range image.

Different parameters have been examined and the best rank one recognition rate achieves 67.5%, which is significantly better than the 3D PCA performance [20].

6 ICP Based Ear Recognition

Besl and McKay's classic ICP algorithm has been implemented [1]. Given a set of source points P and a set of model points X, the goal of ICP is to find the rigid transformation T that best aligns P with X. Beginning with a starting estimate of the registration T_0, the algorithm iteratively calculates a sequence of transformations T_i until the registration converges. In a 3D face image, the eyes and mouth are common places to have holes and spikes. 3D ear images do exhibit some spikes and holes due to oily skin or sensor error, but much less often than in the 3D face images. Therefore in our experiment, an explicit outlier removal step is not used. The iteration number is set as 50, and the cutoff for the distance is 0.0001 mm.

At each iteration, the algorithm computes correspondences by finding closest points, and then minimizes the mean square error between the correspondences. A good initial estimate of the transformation is required, and all scene points are assumed to have correspondences in the model. The centroid of the extracted ear is used as a starting point in our experiments.

6.1 Ear Extraction

Ear extraction is based on the landmark lines located on the original ear images. In the truthwriting process, two lines are used to find the orientation and scaling of the ear [21]. According to that, the mask is rotated and scaled, and applied on the original image. The mask is used to select a subset of the 3D data to be used in matching. Different ear sizes result in variance in the amount of ear data after extraction. Figure 4 shows an example of the original image and mask, along with the appropriate mask and extracted ear. The original profile face scan (640 x 480) is cropped to (116x136) in size for the ear region.

(a) Original Image 1   (b) Original Image 2

(c) Mask of (a)   (d) Extracted ear   (e) Mask of (b)   (f) Extracted ear
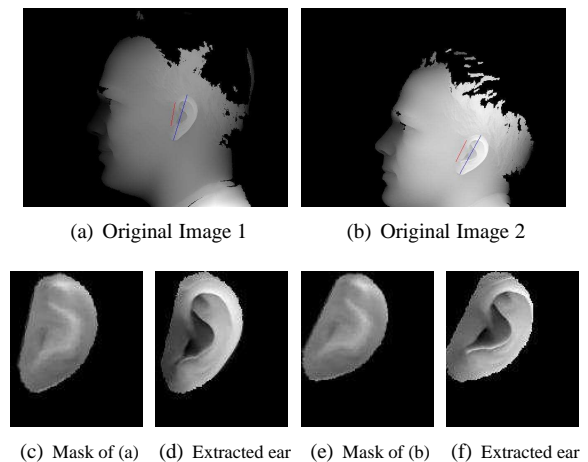
Figure 4. Ear Mask and Cropped 3D Data

Ear Recognition Performance Using 302 Subjects

Legend:
- 3D ICP–Based
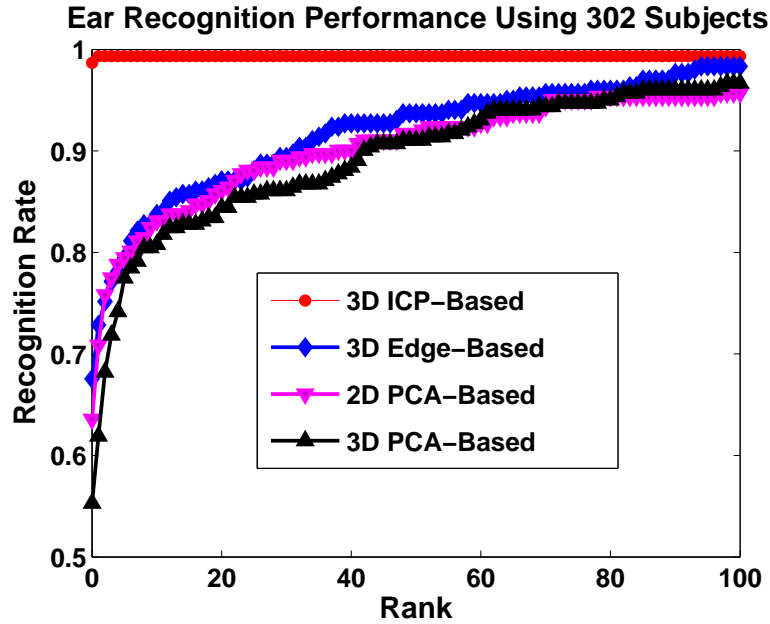- 3D Edge–Based
- 2D PCA–Based
- 3D PCA–Based

Figure 5. Performance of Different Approaches

6.2 Improved ICP

Our initial results using basic ICP reach 84.1% rank one recognition rate. Various refinements were considered, several of which were incorporated into an improved algorithm. The amount of the ear shape used in the gallery and probe representations was adjusted to reduce interference from the background. A step to remove outlier point matches was added to reduce the effects of incorrect correspondences. Our improved algorithm produces substantially better results. Using the 302-person dataset, with a single 3D ear scan as the gallery enrollment for a person, and a single 3D ear scan as the probe for a person, the new algorithm achieves 98.7% rank-one recognition [21].

6.3 Extended Data Size

By including 102 more subjects we acquired from Fall, 2004, we obtain a dataset with 404 subjects, which is so far the largest dataset for the ear biometrics in term of subject size. The image acquisition, landmark selection and ear extraction are as described in the previous section. The ICP-based approach yields 97.5% rank one recognition rate on the 404-person data set.

7 Scaling with Dataset Size

It has been suggested that scaling of performance with dataset size is a critical issue in biometrics [13, 14]. Some

techniques scale better to larger datasets than others. A good algorithm should keep the performance within a reasonable range when the data size expands. Table 1 shows the scalability of the 3D ICP and 2D PCA with different gallery sizes.

	PCA		ICP	
Gallery Size = 25	23	92%	25	100%
Gallery Size = 50	42	84%	49	98%
Gallery Size = 100	75	75%	99	99%
Gallery Size = 150	103	68.7%	149	99.3%
Gallery Size = 200	135	67.5%	199	99.5%
Gallery Size = 302	192	63.6%	298	98.7%

Table 1. PCA and ICP Performance Varied by Data Size

When the gallery size is 25, PCA has 92% rank-one recognition, and ICP is at 100%. As gallery size doubles, there is around a 10% drop in the PCA performance, and when the gallery has 302 subjects, the performance decreases to 63.8%. However, ICP shows a much better scalability. When the gallery size doubles, there is less than 1% drop in ICP performance, and it still reaches 98.7% rank one recognition rate when the gallery size is 302 subjects.

Checking all the incorrect matches for different gallery size, there is one image (shown as Figure 6(b)) that was always mismatched. And of the new incorrect matches appearing in data size 302, two of them (shown as Figure 6(a)

and 6(g)) are new to all the other experiments using different data size, one of them (shown as Figure 6(c)) drops from rank one to rank two when the data size increases from 200 to 302.

(a) Hair Covered   (b) Hair Covered   (c) Hair Covered

(d) 2D of (a)   (e) 2D of (b)   (f) 2D of (c)

(g) Gallery   (h) Probe
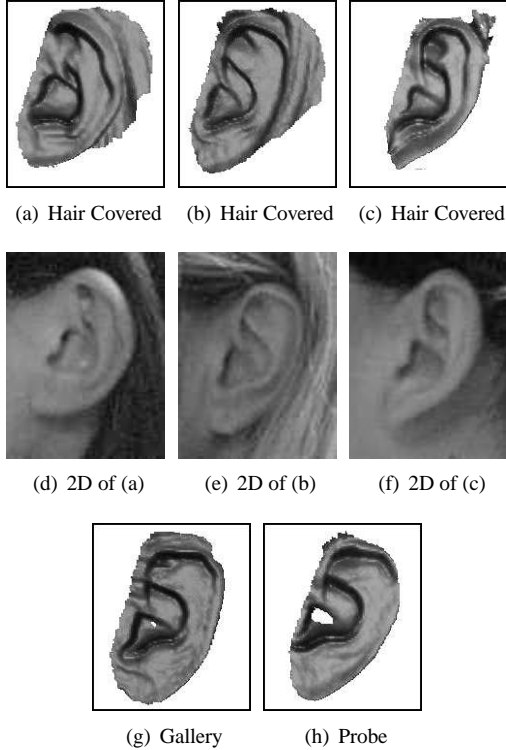
Figure 6. Four Incorrect Matches

8 Statistical Significance Testing

Four single-biometric experiments were explored extensively in the previous sections, represented as a Cumulative Match Characteristic (CMC) Curve in Figure 5. A CMC curve indicates the probability that correct matches appear within some specified candidate size. The faster the CMC curve approaches 1, the better the matching algorithm is. The ICP-based approach has the highest performance, followed by the 3D edge-based approach, then followed by PCA approach on 2D intensity images, and PCA on the 3D range images. Another 3D ear recognition method due to Bhanu and Chen [3] was initially considered but dropped in favor of the other methods described. In order to analyze the performance differences between methods, statistical significance tests were conducted.

The rank one recognition rate can be addressed as a binomial distribution problem. The correct matching rate is the probability of success p and incorrect matching rate is the probability of failure q, where $p + q = 1$. When the sample size becomes larger, the binomial distribution begins to converge to a normal distribution. That is, for a large enough sample size N, a binomial variable X is approximately to $N(Np, Npq)$. Fairly good results are usually obtained when $Npq \geq 3$. Here, $\widehat{p}$ is the proportion of observed correct matches. $\widehat{p}$ value for each method is shown in Table 2. In our circumstance, sample size N = 302, with all $N\widehat{p}\widehat{q} \geq 3$.

	ICP	2D PCA	3D PCA	Edge-based
$\widehat{p}$	0.987	0.636	0.553	0.675
$\widehat{q}$	0.013	0.364	0.447	0.325
$N\widehat{p}\widehat{q}$	3.87	69.91	74.65	66.25

Table 2. Proportion of Observed Correct Matches

Given two methods, with sample size as N_1 and N_2, and proportion of observed correct matches as $\widehat{p}_1$ and $\widehat{p}_2$, the test statistic for $H_0 : p_1 = p_2$ is

$$z = \frac{\widehat{p}_1 - \widehat{p}_2}{\sqrt{(\frac{N_1+N_2}{N_1 N_2})(\frac{X_1+X_2}{N_1+N_2})(1 - \frac{X_1+X_2}{N_1+N_2})}}$$

$$where X_1 = \widehat{p}_1 \times N_1 \ \ and \ X_2 = \widehat{p}_2 \times N_2.$$

Table 3 is constructed using the 0.05 level of significance. It is well known that significance levels from the pairwise comparisons might be misleading. Simply it means that when too many comparisons are carried out, the result may suggest statistically significant differences even if no difference exists [9]. The Bonferroni correction has been used post hoc to determine the significance of multiple tests [9]. It basically multiplies each of the significance levels from the z test by the number of tests performed. If this value is greater than 1, a significance level of 1 is used.

The "reject" in Table 3 refers to rejecting the null hypothesis of no significant difference. The performance of the ICP-based algorithm is statistically significantly better than the other three methods. The edge-based performance is statistically significantly better than the 3D PCA-based method.
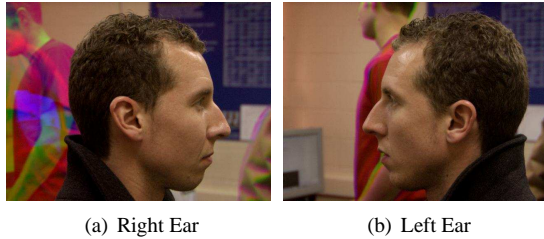
9 Ear Symmetry Experiment

So far the ear data used in our experiments is of good quality, and the gallery and probe images are basically straight-on ear images, of the same ear, on different days. We called this "controlled conditions". It would be very interesting to look at the experimental results from less controlled conditions.

One less controlled approach is matching a mirrored left or right ear, which means that for one subject we enroll his

	Edge	2D PCA	3D PCA
ICP	11.03(Reject)	12.67(Reject)	10.23(Reject)
Edge		1.01(Accept)	3.08(Reject)
2D PCA			2.08(Accept*)

Table 3. Statistical Test of the Difference between Performance, Using 0.05 level of significance. H_0 :: There is no difference in performance between the two methods. (*: after Bonferroni adjustment)

(a) Right Ear   (b) Left Ear

Figure 7. Image acquired for Ear Symmetric experiments

right ear and try to recognize using his left ear. This approach assumes bilateral symmetry of the ear. Two different angles of view have been examined. They are 30 degree off the center and 45 degree off the center. The initial data processing includes landmark ground truth and ear extraction, which are the same as we described in previous sections.

The right ear of the subject is used as the gallery, and the left ear is used as the probe, see Figure 7. For this initial experiment, both ear images are taken on the same day. The results are presented in Table 4.

	number of subjects	Performance
30 degree off	88	90.9%
45 degree off	119	89.1%

Table 4. Ear symmetry Experiments

By analyzing the results, we found that most people's left and right ears are at least close to bilaterally symmetric. But some people's left and right ears have different shapes. Figure 8 shows an example of this. Thus it seems that symmetry-based ear recognition cannot be expected to be as accurate.

10   Summary And Discussion

We have presented experimental results for three different approaches to 3D ear recognition and a PCA-based approach to 2D ear recognition. A fourth algorithm for 3D ear

recognition was also considered [3], but dropped in favor of the other 3D approaches. Our results are based on the largest experimental dataset to date for ear biometrics, with 2D and 3D images acquired for over 300 persons on two different dates. This is the most comprehensive investigation of 3D ear recognition to be reported to date, the largest experimental evaluation of 2D ear recognition, and the first (only) comparison of 2D and 3D ear recognition.

Our 2D PCA ear recognition results are comparable to the state of the art reported in the literature [5]. In our experiments, the ICP-based approach to 3D ear recognition statistically significantly outperforms the other approaches considered for 3D ear recognition, and also statistically significantly outperforms the 2D ear recognition result obtained with a state-of-the-art PCA-based ear recognition algorithm [5]. Thus it appears that ear recognition based on 3D shape is more powerful than based on 2D appearance, although other approaches to 2D ear recognition remain to be considered. It also appears that an ICP-based approach to 3D ear recognition outperforms other approaches that used a range image representation of the 3D data, although again other approaches to 3D recognition using range images could be considered. Interestingly, we find that the ICP-based approach to 3D ear recognition scales quite well with increasing size of dataset. Our current improved ICP algorithm achieves 98.7% rank-one recognition rate on the 302 subject dataset [21], and 97.5% rank-one recognition rate on our expanded 404 subject dataset.

Several topics for additional work seem important and promising. One is to consider methods of improving the computation time required by ICP matching. Another is to further investigate the scalability of 3D ear recognition performance with increased data set size. A third topic is to investigate possible performance improvement by combining 2D and 3D recognition for a multi-modal result [19].

References

[1] P. Besl and N. McKay. A method for registration of 3-D shapes. In *IEEE Trans. Pattern Anal. Machine Intell.*, pages 239–256, 1992.

[2] R. Beveridge, K. She, B. Draper, and G. Givens. Evaluation of face recognition algorithm (release version 4.0). In *URL: www.cs.colostate.edu/evalfacerec/index.html*.

[3] B. Bhanu and H. Chen. Human ear recognition in 3D. In *Workshop on Multimodal User Authentication*, pages 91–98, 2003.

(a) Example 1

(b) Example 1

(c) Right ear)

(d) Mirroed Left ear
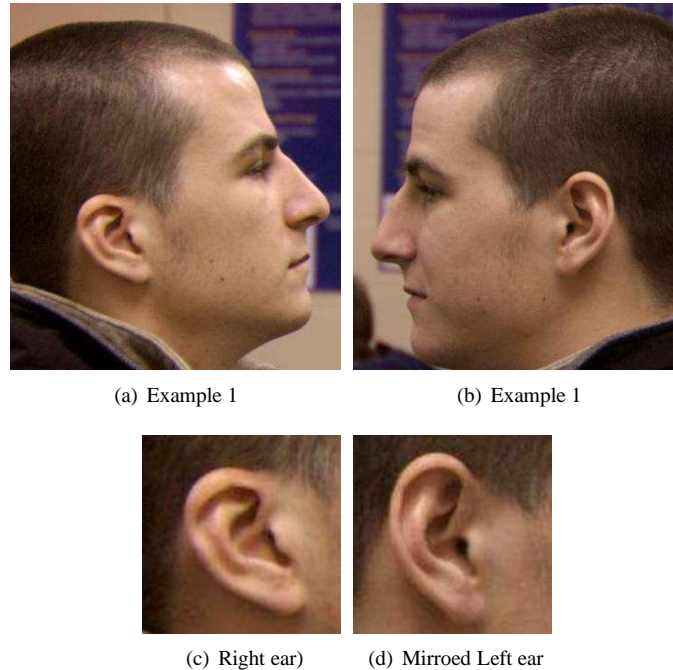
Figure 8. Examples of Asymmetric Ears

[4] M. Burge and W. Burger. Ear biometrics. In *Biometrics: Personal Identification in Networked Society*, pages 273–286. Kluwer Academic, 1999.

[5] K. Chang, K. Bowyer, and V. Barnabas. Comparison and combination of ear and face images in appearance-based biometrics. In *IEEE Trans. Pattern Anal. Machine Intell.*, volume 25, pages 1160–1165, 2003.

[6] K. Chang, K. Bowyer, and P. Flynn. Face recognition using 2D and 3D facial data. In *Workshop on Multimodal User Authentication*, pages 25–32, 2003.

[7] H. Chen and B. Bhanu. Contour matching for 3D ear recognition. In *Seventh IEEE Workshops on Application of Computer Vision*, pages 123–128, 2005.

[8] B. A. Draper, W. S. Yambor, and J. R. Beveridge. Analyzing pca-based face recognition algorithms: Eigenvector selection and distance measures.

[9] W. L. Hays. Thomson Learning, 1996.

[10] D. Hurley, M. Nixon, and J. Carter. Force field energy functionals for image feature extraction. In *Image and Vision Computing Journal*, volume 20, pages 429–432, 2002.

[11] A. Iannarelli. Ear identification. In *Forensic identification series, Fremont, California*. Paramont Publishing Company, 1989.

[12] B. Moreno, A. Sanchez, and J. Velez. On the use of outer ear images for personal identification in security applications. In *IEEE International Carnaham Conference on Security Technology*, pages 469–476, 1999.

[13] P. Phillips, P. Grother, R. Micheals, D. Blackburn, E. Tabassi, and J. Bone. FRVT 2002: Overview and summary. March 2003.

[14] P. Phillips, H. Moon, S. Rizvi, and P. Rauss. The FERET evaluation methodology for face recognition algorithms. In *IEEE Trans. Pattern Anal. Machine Intell.*, volume 22(10), pages 1090–1104, 2000.

[15] K. Pun and Y. Moon. Recent advances in ear biometrics. In *Proceedings of the sixth international conference on Automatic Face and Gesture Recognition*, pages 164–169, May, 2004.

[16] L. Sirovich and M. Kirby. Low dimensional procedure for characterization of human faces. In *Journal of the Optical Society of America*, volume 4 (3), pages 519–524, March 1987.

[17] M. Turk and A. Pentland. Eigenfaces for recognition. In *Journal of Cognitive Neuroscience*, volume 3(1), pages 71–86, 1991.

[18] B. Victor, K. Bowyer, and S. Sarkar. An evaluation of face and ear biometrics. In *16th International Conference of Pattern Recognition*, pages 429–432, Aug. 2002.

[19] P. Yan and K. W. Bowyer. Multi-Biometrics 2D and 3D ear recognition. In *Audio- and Video-based Biometric Person Authentication*, July 2005.

[20] P. Yan and K. W. Bowyer. Ear biometrics using 2D and 3D images. In *Advanced 3D Imaging for Safety and Security*, June 2005.

[21] P. Yan and K. W. Bowyer. ICP-based approaches for 3D ear recognition. In *Biometric Technology for Human Identification II, Proceedings of SPIE*, volume 5779, pages 282–291, March 2005.

[22] T. Yuizono, Y. Wang, K. Satoh, and S. Nakayama. Study on individual recognition for ear images by using genetic local search. In *Proceedings of the 2002 Congress on Evolutionary Computation*, pages 237–242, 2002.